MOL PHARM

MOLECULAR PHARMACOLOGY

DNA-Binding Preferences of Bisantrene Analogues: Relevance to the Sequence Specificity of Drug-Mediated Topoisomerase II Poisoning

CLAUDIA SISSI, LORETTA BOLGAN, STEFANO MORO, GIUSEPPE ZAGOTTO, CHRISTIAN BAILLY, ERNESTO MENTA, GIOVANNI CAPRANICO, and MANLIO PALUMBO

Department of Pharmaceutical Sciences, University of Padova, 35131 Padova, Italy (C.S., L.B., S.M., G.Z., M.P.), INSERM U124 and Laboratoire de Pharmacologie Antitumorale Moléculaire, Centre Oscar Lambret, 59045 Lille, France (C.B.), Boehringer Mannheim Italia, 20052 Monza, Italy (E.M.), and Division of Experimental Oncology B, Istituto Nazionale per lo Studio e la Cura dei Tumori, 20133 Milan, Italy (G.C.)

This paper is available online at http://www.molpharm.org

ABSTRACT

To elucidate structure-activity relationships for drugs that are able to poison or inhibit topoisomerase II, we investigated the thermodynamics and stereochemistry of the DNA binding of a number of anthracene derivatives bearing one or two 4,5-dihydro-1*H*-imidazol-2-yl-hydrazone side chains (characteristic of bisantrene) at different positions of the planar aromatic system. An aza-bioisostere, which can be considered a bisantrene-amsacrine hybrid, was also tested. The affinity for nucleic acids in different sequence contexts was evaluated by spectroscopic techniques, using various experimental conditions. DNA-melting and DNase I footprinting experiments were also performed. The location and number of the otherwise identical side chains dramatically affected the affinity of the test compounds for the nucleic acid. In addition, the new compounds exhibited different DNA sequence preferences, depending on the locations of the dihydroimidazolyl-hydrazone groups, which indicates a major role for the side-chain position in generating specific contacts with the nucleic acid. Molecular modeling studies of the intercalative binding of the 1- or 9-substituted isomers to DNA fully supported the experimental data, because a substantially more favorable recognition of A-T steps, compared with G-C steps, was found for the 9-substituted derivative, whereas a much closer energy balance was found for the 1-substituted isomer. These results compare well with the alteration of base specificity found for the topoisomerase II-mediated DNA cleavage stimulated by the isomeric drugs. Therefore, DNA-binding specificity appears to represent an important determinant for the recognition of the topoisomerase-DNA cleavable complex by the drug, at least for poisons belonging to the amsacrine-bisantrene family.

DNA topoisomerase II is a ubiquitous enzyme that regulates DNA topological features; during its catalytic cycle, it cleaves a DNA duplex, allows the passage of another DNA segment through the cut, and finally reseals the strand breaks (Berger *et al.*, 1996). Eukaryotic type II topoisomerases are the targets of highly effective antitumor drugs such as *m*-AMSA, bisantrene, anthracyclines, and etoposide. The drugs interfere with the DNA breakage-reunion reaction by freezing a transient DNA-enzyme complex in which the DNA strands are cut and covalently linked to the protein (Liu, 1989). The pharmacological activity of these antitumor compounds is thus related to DNA cleavage stimulation in living tumor cells (Pommier, 1993).

Several lines of evidence indicate that topoisomerase II poisons bind to the enzyme/DNA interface at the site of DNA cleavage (Capranico *et al.*, 1997). These drugs are commonly composed of a planar ring system, with DNA-intercalation or -intercalation-like properties, and one or two protruding side chains, which are believed to recognize the enzyme side of the cleavable complex (Osheroff *et al.*, 1994). However, these drugs do not share a unique pharmacophore (Capranico *et al.*, 1997) and can only define a "loose" one, as earlier suggested (Leteurtre *et al.*, 1992). The lack of structural restrictions for the pharmacophore of topoisomerase II poisons can mainly be ascribed to receptor heterogeneity, which is determined by the variability of the local nucleic acid sequence at the enzyme/DNA interface. This is reflected in marked differences of cleavage patterns observed in sequencing gels and local base preferences among the different classes of chemical poisons (Capranico *et al.*, 1990, 1993; Pommier *et al.*, 1991).

ABBREVIATIONS: *m*-AMSA, 4′-(9-acridinylamino)methanesulfon-*m*-anisidide; 9-IHA, anthracene-9-carboxaldehyde-(4,5-dihydro-1*H*-imidazol-2-yl)hydrazone hydrobromide; aza-9-IHA, 9-acridinecarboxaldehyde-(4,5-dihydro-1*H*-imidazol-2-yl)hydrazone hydrobromide; 1-IHA, anthracene-1-carboxaldehyde-(4,5-dihydro-1*H*-imidazol-2-yl)hydrazone hydrobromide; 1,4-IHA, anthracene-1,4-dicarboxaldehyde-(4,5-dihydro-1*H*-imidazol-2-yl)dihydrazone hydrobromide; DS, DNA binding specificity; TS, topoisomerase II-mediated sequence specificity; T_m, melting temperature.

In previous attempts to define the structural determinants of this important family of anticancer agents, we demonstrated that, although many chemically unrelated poisons can stimulate DNA cleavage in the presence of topoisomerase II, only compounds sharing common steric and electronic features can trap the enzyme at the same nucleic acid sites (Capranico *et al.*, 1994). This is the case for bisantrene and *m*-AMSA, which have identical A+1 base requirements for topoisomerase II-mediated DNA cleavage stimulation. In fact, a remarkable similarity in space occupancy and charge distribution was demonstrated for the two compounds, which might account for the equivalent base requirements (Capranico *et al.*, 1994). Stimulated by these findings, we recently investigated a number of bisantrene congeners, including a 10-aza-bioisoster, bearing the same 4,5-dihydro-1*H*-imidazol-2-yl-hydrazone side chain at positions 1, 4, or 9 of anthracene (Capranico *et al.*, 1998). Moving the bisantrene side chain along the planar ring system (from C9 and C5 to C1 and C4) dramatically affected the base preference and intensity patterns of poison-stimulated DNA cleavage. In contrast, switching the planar aromatic systems of bisantrene and *m*-AMSA did not substantially alter the sequence specificity of drug action. Base preferences at the cleavage site are reported in Table 1. Indeed, a common pharmacophore was shared by bisantrene, *m*-AMSA, and the 9-substituted analogues, whereas the 1-substituted regioisomer showed radically changed pharmacophoric properties.

Because topoisomerase poisons, including *m*-AMSA, likely interact at the protein/DNA interface (Freudenreich and Kreuzer, 1994; Capranico *et al.*, 1997), their DNA-binding activity can be affected by the structural and chemical changes induced by protein/nucleic acid contacts. In the case of anthracyclines, the base preferences exhibited by the drug for naked DNA and for the topoisomerase II-DNA complex are different, indicating that alterations of the drug interaction with the double helix occur in the ternary complex. Amsacrine, on the other hand, shows the same (5′-TA) dinucleotide preference for binding to protein-free DNA and for stabilizing the enzyme-DNA complex (Chen *et al.*, 1988; Pommier *et al.*, 1991). Hence, a thorough understanding of the structural and functional aspects of the effects of the protein on poison-DNA interactions is still missing. In this connection, we were interested in investigating the DNA-binding affinity and specificity of the series of bisantrene/*m*-AMSA

congeners shown in Fig. 1 and comparing them with the sequence preferences found in the topoisomerase II-poisoning experiments (Capranico *et al.*, 1998).

We show that not only the affinity for the nucleic acid is affected; the DS is also dramatically modified upon movement of the side-chain groups along the anthracene ring system. Most interestingly, the changes in specificity exhibited by structural isomers in the binary drug-DNA system precisely correspond to the specificity changes observed for enzyme-mediated DNA cleavage. This information could facilitate further elucidation of the details of the mechanism of action of topoisomerase poisons and will be valuable in the rational design of novel poisons with a predefined site selectivity for DNA cleavage.

Experimental Procedures

Materials. *m*-AMSA and bisantrene were obtained from the Drug Synthesis and Chemistry Branch, National Cancer Institute (Bethesda, MD), and from Lederle, respectively. The imidazolyl-hydrazone compounds were synthesized as described elsewhere (Zagotto *et al.*, 1998). All compounds used were stored at −20° in dimethylsulfoxide or deionized water and were diluted in deionized water before use.

The three natural DNAs, from calf thymus (highly polymerized sodium salt), *Clostridium perfringens,* and *Micrococcus lysodeikticus*, as well as pBR322 plasmid and double-stranded polynucleotides, were purchased from Pharmacia (Milan, Italy) or Sigma Chemical Co. (St. Louis, MO). Their concentrations were determined by applying the molar extinction coefficients reported in the literature (Grant *et al.*, 1968; Wells *et al.*, 1970). DNAs and polynucleotides were used without purification except for calf thymus DNA, which was deproteinized twice with sodium dodecyl sulfate. After purification, the protein content was <0.2% and did not interfere with the present results. All DNAs were dialyzed at 4° against Tris or BPE buffer (6 mM Na_2HPO_4, 2 mM NaH_2PO_4, 1 mM EDTA, pH 7.1) before use.

Single-stranded DNA (ϵ = 8350 M^{-1} cm^{-1}) was provided by Crinos S.p.A. (Villaguardia, Italy). DNA topoisomerase II was purified from the nuclei of murine P388 cells and stored as described (De Isabella *et al.*, 1990). Simian virus 40, restriction enzymes, the DNA-modify-

TABLE 1
Base preferences at the site of topoisomerase II-mediated DNA cleavage stimulated by the test poisons

Position from the cleaved bond[a]	Base	−log P[b]		
		m-AMSA	9-IHA	1-IHA
−1	A	−0.4	−0.9	−0.5
	G	+0.6	−0.4	−0.2
	C	+0.4	+2.0	+1.2
	T	−0.5	−0.5	−0.5
+1	A	+2.7	+2.5	+1.1
	G	−0.6	−0.6	+0.5
	C	−0.6	+0.3	−0.7
	T	−0.9	−1.8	−1.0

[a] Enzyme-mediated cleavage occurs between positions −1 and +1.
[b] Negative logarithm of the probability of observing that deviation or more as either an excess (positive numbers) or deficiency (negative numbers), relative to the expected base frequency in simian virus 40 DNA. Weakly and strongly stimulated sites were analyzed. The numbers of sites analyzed were 126, 66, and 37 for *m*-AMSA, 9-IHA, and 1-IHA, respectively.
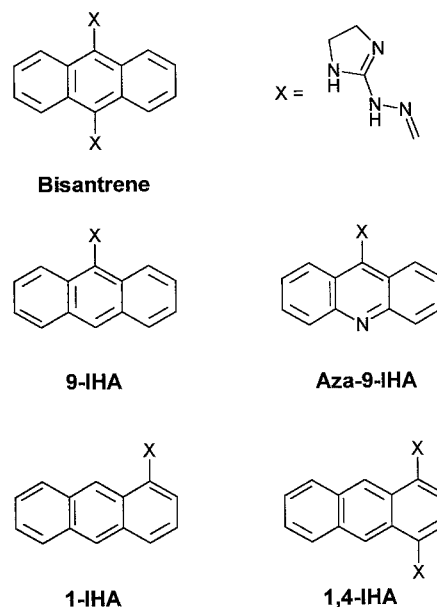

Fig. 1. Chemical structures of the test drugs.

ing enzymes, agarose, and acrylamide were from GIBCO-BRL (Gaithersburg, MD) or from New England Biolabs (Beverly, MA).

Nucleoside triphosphates labeled with ^{32}P ([α-^{32}P]dATP and [γ-^{32}P]ATP; 3000 Ci/mmol) were obtained from Amersham (Milan, Italy). The restriction endonucleases AvaI, EcoRI, HindIII, and PvuII, alkaline phosphatase, T4 polynucleotide kinase, and avian myeloblastosis virus reverse transcriptase were purchased from Boehringer (Mannheim, Germany) and were used according to the protocol recommended by the supplier, in the activity buffer provided. All other chemicals were analytical grade reagents, and all solutions were prepared using doubly deionized, filtered (Millipore filter) water.

Stability of the test drugs in aqueous media. All compounds were stable in aqueous solution at the working concentrations and did not undergo self-aggregation phenomena up to at least 100 μM. A notable exception was 1,4-IHA, whose molar extinction coefficient decreased with increasing concentration. This phenomenon has been described for molecules containing hydrophobic planar systems that could stack on each other, including bisantrene and mitoxantrone. The dependence of the extinction coefficient on the drug concentration was investigated at different ionic strengths. The experimental

Fig. 2. Examples of spectrophotometric (A) and fluorometric (B) titration experiments for the binding of test drugs to double-stranded DNA from calf thymus, in ETN buffer (0.1 M, pH 7.0). *Curve 1*, free drug; *curve 2*, totally bound drug. A, 1-IHA (15.3 μM); B, aza-9-IHA (1.6 μM).

data obtained by spectroscopic titrations were consistent with a model of indefinite aggregation (Schwartz et al., 1970), which takes into account aggregation processes beyond a simple monomer-dimer equilibrium. As could be anticipated, considering the presence of protonated side chains, with increasing ionic strength the drug charge becomes shielded, which reduces the repulsive effect and stabilizes the aggregates. An association constant value of approximately 10^4 M^{-1} was found.

DNA binding studies. Measurements were carried out at 25° in ETN buffer (1 mM EDTA, 10 mM Tris, pH 7.0, with NaCl to obtain the desired ionic strength). Binding was monitored spectrophotometrically or fluorometrically, in the ligand absorption or emission region, respectively, after addition of scalar amounts of DNA to a freshly prepared drug solution. To avoid large systematic inaccuracies resulting from experimental errors in extinction coefficients or fluorescence quantum yield, the range of bound drug fractions was 0.15–0.85. Data were evaluated according to the equation of McGhee and Von Hippel (1974) for noncooperative ligand-lattice interactions,

$$r/m = K_i(1 - nr)^n/[1 - (n - 1)r]^{n-1}$$

where r is the molar ratio of bound ligand to DNA, m is the free ligand concentration, K_i is the intrinsic binding constant, and n is the exclusion parameter. Spectroscopic measurements were made with a Perkin-Elmer Lambda 5 apparatus and a MPF66 fluorometer, both equipped with a Haake F3-C thermostat.

T_m studies. Melting curves were measured using a Uvikon 943 spectrophotometer coupled to a Neslab RTE111 cryostat. For each series of measurements, 12 samples were placed in a thermostatically controlled cell-holder (path length, 10 mm), and the quartz cuvettes were heated by circulating water. The measurements were made in BPE buffer (pH 7.1). The temperature inside the cuvette was monitored by using a thermocouple in contact with the solution. The absorbance at 260 nm was measured over the range of 20–100°, with a heating rate of 1°/min. The T_m was taken as the midpoint of the hyperchromic transition.

DNA-unwinding assays. Plasmid DNA (pBR322) was incubated for 30 min with increasing concentrations (0–100 μM) of 9-IHA, aza-9-IHA, and 1-IHA. Aliquots containing 400 ng of DNA (10 μl) were then loaded onto 1% agarose gels, after addition of 2 μl of loading buffer (0.01% bromphenol blue, 0.01% xylene cyanol, 40% sucrose). Gels were run in TBE buffer (89 mM Tris-borate, pH 8.3, 1 mM EDTA) at 10 V/cm. The gels were then stained with ethidium bromide (0.5 mg/liter) and scanned using a BioRad Gel Doc 1000 system.

DNA purification and labeling. Plasmid pBS (Stratagene) was isolated from *Escherichia coli* by a standard sodium dodecyl sulfate-sodium hydroxide lysis procedure and was purified by banding in CsCl-ethidium bromide gradients. Ethidium was removed by several isopropanol extractions followed by exhaustive dialysis against Tris-EDTA buffer. The purified plasmid was then precipitated and resuspended in appropriate buffer before digestion with the restriction
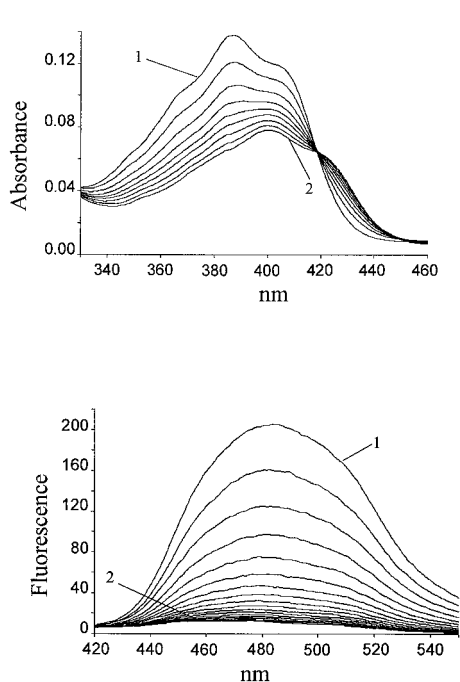
TABLE 2
Thermodynamic binding properties of test compound binding to calf thymus DNA in ETN buffer at different ionic strengths (pH 7.0, 25°)
The values of the exclusion parameter n were close to 2 base pairs in all cases. They were slightly less than 2 for 1-IHA at low salt concentrations (0.022–0.1 M); this fact probably reflects modest external stacking of the drug when bound to DNA.

Compound	K_i ($\times 10^{-4}$)[a]				m'[b]	$-\Delta G°$[c]
	0.022 M[d]	0.10 M	0.25 M	0.50 M		
			M^{-1}			kcal/mol
9-IHA	59.5 ± 2.8	17.6 ± 1.9	4.64 ± 0.4	ND[e]	1	5.6
Aza-9-IHA	61.7 ± 2.8	18.0 ± 1.8	6.59 ± 0.5	ND	1	5.8
1-IHA	17.6 ± 1.6	5.61 ± 0.5	2.35 ± 0.2	0.78 ± 0.1	1	5.0
Bisantrene	ND	660 ± 31	113 ± 4.8	29.1 ± 2.0	2	6.6

[a] Intrinsic binding constant.
[b] m' is the number of ionic contacts per complex unit, calculated from the slope $\delta\log K_i/\delta\log$ (ionic strength) (Fig. 5).
[c] Interaction free energy corrected for the electrostatic contribution.
[d] Ionic strength.
[e] ND, not determined.

enzymes. The 265-base pair DNA fragment was prepared by 5′-³²P-end-labeling of the *Eco*RI/alkaline phosphatase-treated plasmid using [γ-³²P]ATP (6000 Ci/mmol) and T4 polynucleotide kinase, followed by treatment with *Pvu*II. The digestion products were separated on a 6% polyacrylamide gel under native conditions in TBE buffer. After autoradiography, the band of DNA was excised, crushed, and soaked in elution buffer (500 mM ammonium acetate, 10 mM magnesium acetate) overnight at 37°. This suspension was filtered through a Millipore 0.22-μm filter, and the DNA was precipitated with ethanol. After washing with 70% ethanol and vacuum drying of the precipitate, the labeled DNA was resuspended in 10 mM Tris (adjusted to pH 7.0) containing 10 mM NaCl.

DNase I footprinting experiments. Experiments were performed essentially as previously described (Bailly and Waring, 1995). Briefly, reactions were conducted in a total volume of 10 μl. Samples (3 μl) of the labeled DNA fragment were incubated with 5 μl of the buffer solution containing the ligand at the appropriate concentration. After 30 min of incubation at 37° to ensure equilibration of the binding reaction, the digestion was initiated by the addition of 2 μl of a DNase I solution, the concentration of which was adjusted to yield a final enzyme concentration of approximately 0.01 unit/ml in the reaction mixture. After 3 min, the reaction was stopped by freeze-drying. Samples were lyophilized and resuspended in 5 μl of an 80% formamide solution containing tracking dyes. The DNA samples were then heated at 90° for 4 min and chilled on ice for 4 min before electrophoresis.

Electrophoresis and quantitation by storage phosphor imaging. DNA cleavage products were resolved by polyacrylamide gel electrophoresis under denaturing conditions (0.3-mm thick gels, 8% acrylamide containing 8 M urea). After electrophoresis (approximately 2.5 hr at 60 W and 1600 V in TBE buffer; BRL sequencer model S2), gels were soaked in 10% acetic acid for 10 min, transferred to Whatman 3MM paper, and dried under vacuum at 80°. A Molecular Dynamics 425E PhosphorImager was used to collect data from the storage screens exposed to dried gels overnight at room temperature. Base-line-corrected scans were analyzed by integrating all densities between two selected boundaries using ImageQuant version 3.3 software. Each resolved band was assigned to a particular bond within the DNA fragment by comparison of its position with those of sequencing standards generated by treatment of DNA with dimethylsulfate (guanine) and/or formic acid (guanine plus adenine), followed by piperidine-induced cleavage at the modified bases in the DNA.

Molecular modeling. This study involved the use of the consensus dinucleotide intercalation geometries d(ApT) and d(GpC), which were initially derived from the crystal structures of adriamycin (Frederick *et al.*, 1990) and proflavine (Neidle *et al.*, 1988) intercalation complexes, respectively. The d(ApT) and d(GpC) intercalation sites were located at the center of a decanucleotide duplex having the sequence d(5′-ATATA-3′)$_2$ and d(5′-GCGCG-3′)$_2$. Decamers in the

B-form were built using the nucleic acid builder function of the HyperChem software program (release 4.5; Hypercube Inc., Gainesville, FL). Both decanucleotides were minimized using the Amber all-atom force field (Weiner *et al.*, 1986) of the Macromodel 5.0 molecular modeling package (Mohamadi *et al.*, 1990), until the root mean square of the conjugate gradient was <0.05 kcal/mol/Å. The dielectric constant was assumed to be distance independent, with a magnitude of 4.

1-IHA and 9-IHA geometries were fully optimized, without geometry constraints, using RHF/3–21G(*) (Hehre *et al.*, 1986) *ab initio* calculations Vibrational frequency analysis was used to characterized the minima stationary points (zero imaginary frequencies). The Spartan software package (release 4.2; Wavefunction Inc., Irvine, CA) was used for all quantum mechanical calculations.

1-IHA and 9-IHA structures were rigidly docked into the intercalation site without relaxing the atomic coordinates of either ligand or nucleotide. The side-chain groups were alternatively located in the minor groove or in the major groove. The resulting DNA-ligand intercalated complexes were subjected to Amber all-atom energy minimization until the root mean square of the conjugate gradient was <0.01 kcal/mol/Å. Charges for the ligands were imported from the Spartan output files.

The interaction energy values were calculated as follows: $\Delta E_{\text{intercalation}} = E_{\text{complex}} - (E_{\text{L}} + E_{\text{oligomer}})$. These energies do not correspond to the real energetic value in a rigorous thermodynamic way. They can only be compared with each other in terms of more or less favorable states. All molecular modeling calculations were performed with an IBM RISC System 6000 model 250 Unix workstation.

Results

Thermodynamics of DNA Binding

Spectroscopic studies. Upon addition of DNA (polynucleotide) solutions, all test compounds exhibited dramatic changes in their spectroscopic properties. In particular, the fluorescence of 9-IHA and aza-9-IHA was progressively quenched (Fig. 2B), and the absorption spectrum of 1-IHA underwent a bathochromic and hypochromic shift, generating an isosbestic point (Fig. 2A). The case of 1,4-IHA deserves additional comment. The drug tends to aggregate to a remarkable extent (see Experimental Procedures) and was very effective in inducing DNA condensation and precipitation even at the lowest binding ratios examined. Therefore, a quantitative evaluation of the DNA binding constants for this compound was not possible, but it can be safely stated that this drug exhibits a very high affinity for the nucleic acid under the experimental conditions used.

Analysis of the binding data yielded the thermodynamic
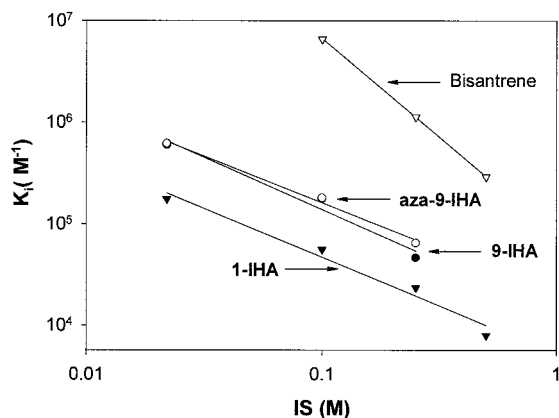
Fig. 3. Dependence of the binding constant K_i for the test congeners on ionic strength (IS).

TABLE 3
Binding affinities of the test compounds for single-stranded DNA in ETN buffer (0.1 M, pH 7.0, 25°)
The values of the exclusion parameter *n* were always close to 2 bases.

Compound	K_i (×10⁻⁴)^a
	M^{-1}
9-IHA	37.9 ± 3.0
Aza-9-IHA	12.2 ± 0.9
1-IHA	5.9 ± 0.5
Bisantrene	101.2 ± 7.9

^{a} Intrinsic binding constant.

---

parameters reported in Table 2. The novel compounds exhibited binding affinities on the order of 10^5 M^{-1}, with 9-IHA and aza-9-IHA closely resembling each other and 1-IHA showing a 3-fold lower interaction constant, compared with its isomeric congeners. On the other hand, in agreement with previous reports (Denny and Wakelin, 1987; Wunz et al., 1990), bisantrene showed an outstanding ability to form a complex with DNA. Its binding constant at the various experimental conditions was always almost 2 orders of magnitude greater than the constants of monosubstituted congeners.

Considering the charged nature of the side chains of the drugs, the use of different ionic strengths allowed us to evaluate the electrostatic contribution of ionic interactions to the binding process. All drugs showed a linear relationship of log K_i versus log ionic strength (Fig. 3). Using the polyelectrolyte theory adapted to nucleic acids (Record et al., 1978), it was possible to confirm that one charged interaction occurs in the DNA binding of compounds bearing one dihydroimidazolyl side chain ($m' = 1$), whereas two ion pairs effectively neutralize the negative charge density of the nucleic acid in the case of bisantrene ($m' = 2$). In addition, the interaction free energy corrected for the electrostatic interactions could be evaluated according to the following equation (Record et al., 1978):

$$\ln K_i = \ln K° + m'\xi^{-1}\ln(\gamma \pm \delta) - m'\psi\ln[\text{M}^+]$$

where K_i is the binding constant calculated at a given salt concentration, $K°$ is the constant corrected for ion release, ψ, ξ, and δ are known physical parameters (0.88, 4.2, and 0.56, respectively, for native DNA), and $\gamma_\pm$ is the activity coefficient of M$^+$, the added salt, at the given ionic strength. Bisantrene exhibits the most effective binding (even neglecting electrostatic contacts), followed by the 9-substituted compounds and finally by 1-IHA.

Mode of interaction. Compounds 9-IHA, aza-9-IHA, and 1-IHA were examined for their abilities to affect the electrophoretic mobility of supercoiled plasmid DNA. As expected from the close structural similarities with the parent drugs, which are well known intercalators, all of them caused a progressive decrease of plasmid mobility in the gel, followed by a leveling off and finally an increase with increasing drug concentration (data not shown). This behavior is clearly indicative of an intercalating mechanism of binding for the test drugs.

Binding to single-stranded DNA. To evaluate the effect of DNA structure on the binding efficiency of the test drugs, we also determined the affinity constants with single-stranded nucleic acid. The quantitative data are reported in Table 3. Interestingly, bisantrene congeners retained a remarkable capacity for binding to the single-stranded structure. In comparison with the K_i values found for double-stranded DNA, 9-IHA showed a 2-fold increase, 1-IHA maintained the same values, and aza-9-IHA exhibited a modest reduction. On the other hand, bisantrene, although undergoing a 6-fold reduction in K_i, still exhibited an affinity constant of the order of 10^6 M^{-1}.

Melting experiments. Effective intercalating drugs are well known for their ability to shift the T_m of double-stranded DNA to higher values (Foye et al., 1986). Although increases in T_m cannot be immediately correlated with binding stability, high ΔT_m values are indicative of tight interactions. The results of melting experiments performed with the test drugs using a number of natural and synthetic DNAs are reported in Table 4. No useful data could be obtained with poly(dG-dC) because of the very high T_m ($\approx 97°$) exhibited by the polynucleotide. Values of ΔT_m always increased with increasing drug concentration and were as high as 44° in the case of 1,4-IHA, whereas they never exceeded 21° for the monosubstituted congeners. Considering that ΔT_m values for bisantrene did not exceed 42°, this confirms the outstanding DNA-binding efficiency of the 1,4-disubstituted analogue, in agreement with the results presented above.

In addition, and again in agreement with the thermodynamic data, 9-IHA and its aza-analogue showed very similar melting effects with all DNAs tested. Moreover, 1-IHA was always less effective than 9-IHA (and aza-9-IHA) in increasing the T_m, which confirms its lower binding affinity.

Regarding the possible effects of DNA composition, it should be emphasized that the various DNAs used in these experiments exhibit considerably different T_m values (ranging from 35° to 75°). It is important to remember that the DNA binding constant is temperature dependent (in general, it decreases with increasing temperature), so that at given drug and DNA concentrations the amount of DNA-bound drug is different at different temperatures. In particular, for

TABLE 4
Effects of the test compounds on the melting of polydeoxyribonucleotides and natural DNAs in BPE buffer (pH 7.1)

The T_m values for native DNA and polynucleotides were 41.1° for poly(dA-dT) · poly(dA-dT), 34.7° for poly (dI-dC) · poly(dI-dC), 66.7° for poly(dA-dC) · poly(dG-dT), 58.5° for poly(dA-dG) · poly(dC-dT), 58.5° for Clostridium DNA (72% AT), 65.6° for calf thymus DNA (42% AT), and 74.7° for Micrococcus DNA (26% AT).

| | \(\Delta T_m\) | | | | | | | | | | | |
| | 9-IHA | | | Aza-9-IHA | | | 1-IHA | | | 1,4-IHA | | |
Compound	2 μM[a] (0.1)[b]	5 μM (0.25)	10 μM (0.5)	2 μM (0.1)	5 μM (0.25)	10 μM (0.5)	2 μM (0.1)	5 μM (0.25)	10 μM (0.5)	2 μM (0.1)	5 μM (0.25)	10 μM (0.5)
						degrees						
Poly(dA-dT) · (dA-dT)	11.8	16.5	21.3	10.8	15.6	18.4	8.9	14.7	19.5	33.1	39.9	43.7
Poly(dI-dC) · (dI-dC)	7.8	12.8	13.7	7.8	10.6	12.5	2.9	5.8	8.7	27.1	33.9	37.7
Poly(dA-dC) · (dG-dT)	2.0	3.0	4.9	1.0	2.0	3.9	1.0	2.0	2.9	15.5	22.0	24.7
Poly(dA-dG) · (dC-dT)	4.6	7.5	10.0	2.8	8.4	10.3	1.6	2.1	3.2	8.8	12.6	15.8
Clostridium perfringens DNA	5.4	9.1	9.7	4.0	10.0	11.3	1.9	4.8	6.7	19.4	25.2	30.4
Calf thymus DNA	3.8	4.7	5.9	1.9	2.9	3.8	0.5	1.0	2.1	15.5	22.1	26.3
Micrococcus lysodeikticus DNA	4.2	5.4	7.7	0.8	1.0	1.0	1.4	2.4	2.9	10.1	14.2	≥16

[a] Drug concentration.
[b] Drug/DNA ratio.

exothermal binding reactions, DNAs with low T_m values [e.g., poly(dA-dT)] show greater T_m effects than do DNAs with high T_m values (e.g., *M. lysodeikticus* DNA). Indeed, to properly assess base preferences, one should be able to monitor melting effects at constant levels of drug binding [rather than at constant concentrations of total (bound plus free) drug].
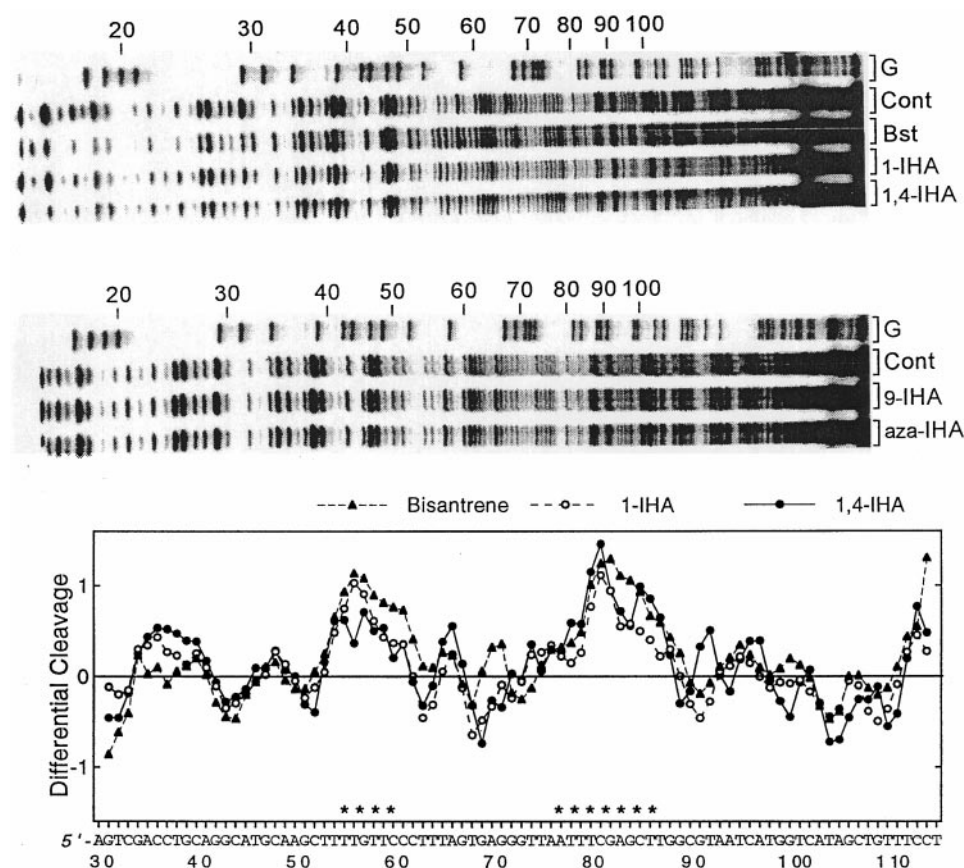
TABLE 5

Effects of DNA sequence on binding affinity in ETN buffer (0.1 M, pH 7.0, 25°)

The values of the exclusion parameter n were close to 2 base pairs in all cases.

Compound	K_i ($\times 10^{-4}$)[a]		
	Calf thymus DNA	Poly(dA-dT)	Poly(dG-dC)
		M^{-1}	
9-IHA	17.6 ± 1.9	31.0 ± 2.1	5.6 ± 0.5
Aza-9-IHA	18.0 ± 1.8	35.4 ± 2.2	16.8 ± 1.3
1-IHA	5.61 ± 0.5	12.5 ± 1.1	10.1 ± 1.0

[a] Intrinsic binding constant.

DNA Sequence Selectivity

Spectroscopic measurements. Spectrophotometric and fluorometric methods were used to evaluate the affinities of the test drugs for DNAs with different base compositions. The results are reported in Table 5. 9-IHA and aza-9-IHA demonstrated a clear preference for A-T steps. In contrast, 1-IHA was able to bind to AT- or GC-rich DNAs almost equally well, losing the selectivity shown by the 9-substituted congeners. As expected from previous reports on intercalating ligands, binding of the test compounds to poly(purine)·poly(pyrimidine) sequences was substantially disfavored (data not shown).

DNase I footprinting experiments. Footprinting studies were performed to gain further insight into the sequence preferences exhibited by the tested anthracene derivatives. A representative example is shown in Fig. 4. The gel and the corresponding differential cleavage plots reveal that the nuclease activity was only slightly affected in the presence of 1-IHA and 1,4-IHA (20 μM each). Bisantrene exhibited a more pronounced effect (it was used at 5 μM), whereas both 9-IHA and aza-9-IHA showed absolutely no effects even at

Fig. 4. DNase I footprinting with the 5′-end-labeled 265-mer *Pvu*II-*Eco*RI restriction fragment cut from the plasmid pBS, in the presence of 5 μM bisantrene (*Bst*) or its derivatives (20 μM each). Control tracks (*Cont*) contained no drug. Guanine-specific sequence markers (*G*) obtained by treatment of the DNA with dimethylsulfate, followed by piperidine cleavage, were also run. *Numbers at the top of the gels* refer to the numbering scheme of the fragment. The differential cleavage plots compare the susceptibility of the fragment to DNase I cutting in the presence of bisantrene, 1-IHA, and 1,4-IHA. Negative values correspond to a ligand-protected site and positive values represent enhanced cleavage. The *vertical scale* is in units of ln (f_a) − ln (f_c), where f_a is the fractional cleavage at any bond in the presence of the drug and f_c is the fractional cleavage of the same bond in the control. Only the region of the restriction fragment analyzed by densitometry is shown. ★, Sites of drug-induced enhanced reactivity toward DNase I.

TABLE 6

Calculated and experimental binding energy values for the intercalation process (L + oligomer ⇌ L-oligomer)

L	Oligomer	E_L	$E_{oligomer}$	$E_{complex}$	$\Delta E_{intercalation}$[a]	ΔG[b]
		kcal/mol	*kcal/mol*	*kcal/mol*	*kcal/mol*	*kcal/mol*
9-IHA	d(A-T/T-A)$_5$	−21.7	−1790.9	−1860.7	−48.1	−7.5
1-IHA	d(A-T/T-A)$_5$	−5.9	−1790.9	−1825.9	−29.1	−6.9
9-IHA	d(G-C/C-G)$_5$	−21.7	−2001.8	−2049.3	−25.8	−6.4
1-IHA	d(G-C/C-G)$_5$	−5.9	−2001.8	−2039.6	−31.9	−6.8

[a] $\Delta E_{intercalation} = E_{complex} - (E_L + E_{oligomer})$.
[b] Experimental values measured at 25°, using the binding constants of Table 5.

concentrations as high as 100 μM (gel not shown). Quantitative analysis of the footprinting gels (the one shown in Fig. 4 and others with various DNA fragments) provided two interesting pieces of information. First, in the presence of the 1-substituted derivatives, but not with the 9-substituted congeners, the DNase I cleavage was enhanced at sequences containing contiguous A-T pairs. Both bisantrene and 1,4-IHA frequently promoted DNase I cleavage at oligopurine·oligopyrimidine tracts; conversely, they slightly reduced the cleavage activity at alternating purine-pyrimidine sequences. The preference for mixed purine-pyrimidine sequences is also apparent from the T_m measurements. Indeed, much higher ΔT_m values were obtained with poly (dA-dC)·poly(dG-dT) than with poly(dA-dG)·poly(dC-dT) in the presence of 1,4-IHA (Table 4). Second, the sequences where cleavage by the nuclease was slightly reduced were neither GC- nor AT-rich. In most cases, they contained at least one 5'-GT-AC or 5'-TG-CA dinucleotide step. The footprinting data reinforce the conclusion, drawn from the spectroscopic measurements, that 1-IHA can bind to both AT- and GC-containing sequences. The lack of effective interference of the 9-substituted drugs with the cleavage of DNA by the enzyme was anticipated. It might be attributable to the relatively low affinity of the drugs and/or to the fast on and off kinetics. It is well known that amsacrine and related 9-aminoacridine analogues do not interfere with the DNase I cleavage reaction (Wakelin *et al.*, 1990; Bailly *et al.*, 1992; Crenshaw *et al.*, 1995). Although DNase footprinting and topoisomerase stimulation experiments were performed with different DNA fragments, a comparison between them is significant because it is based on a statistical analysis.

Molecular Modeling Studies

Docking experiments were performed to calculate the energy changes and optimal geometries corresponding to the intercalative binding of 9-IHA and 1-IHA to A-T and G-C steps in a double-helical structure. In agreement with the binding experiments reported above, only alternating purine-pyrimidine steps were considered. In all cases, intercalation from the minor groove was preferred by 6–8 kcal/mol. The energy balance for the most favorable binding of 9-IHA and 1-IHA to A-T and G-C base pairs is presented in Table 6.

Interestingly, an effective sequence discrimination appears to operate for 9-IHA; an energy difference of 22 kcal/mol was observed between intercalation into the more favored A-T step and that into the less preferred G-C step. In contrast, 1-IHA showed substantially reduced selectivity, with G-C steps being slightly favored (<3 kcal/mol) over A-T steps. It should be emphasized that the calculated interaction energy values were approximated; they do not take into account entropy changes and solvation effects, which might provide relevant contributions to the binding process. It is, however, encouraging that the rank of calculated intercalation energies corresponds satisfactorily to the rank of experimentally determined free energies of binding (Fig. 5).

The structures corresponding to the most stable intercalation geometries of 9-IHA and 1-IHA are presented in Figs. 6
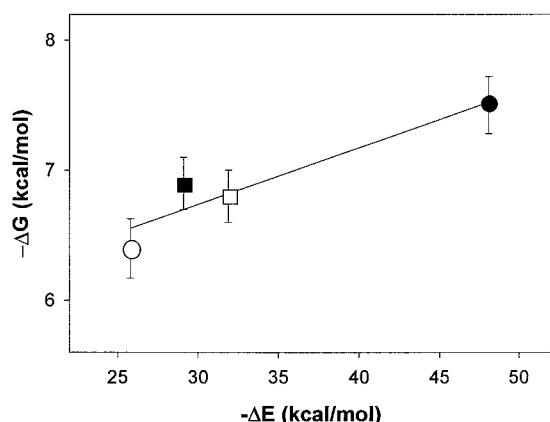
Fig. 5. Relationship between the calculated energy of intercalation (ΔE) and the experimental free energy of binding (ΔG) corresponding to the interaction of 9-IHA (*circles*) and 1-IHA (*squares*) with A-T (*closed symbols*) and G-C (*open symbols*) polynucleotides.

TA- 9-IHA

TA- 1-IHA
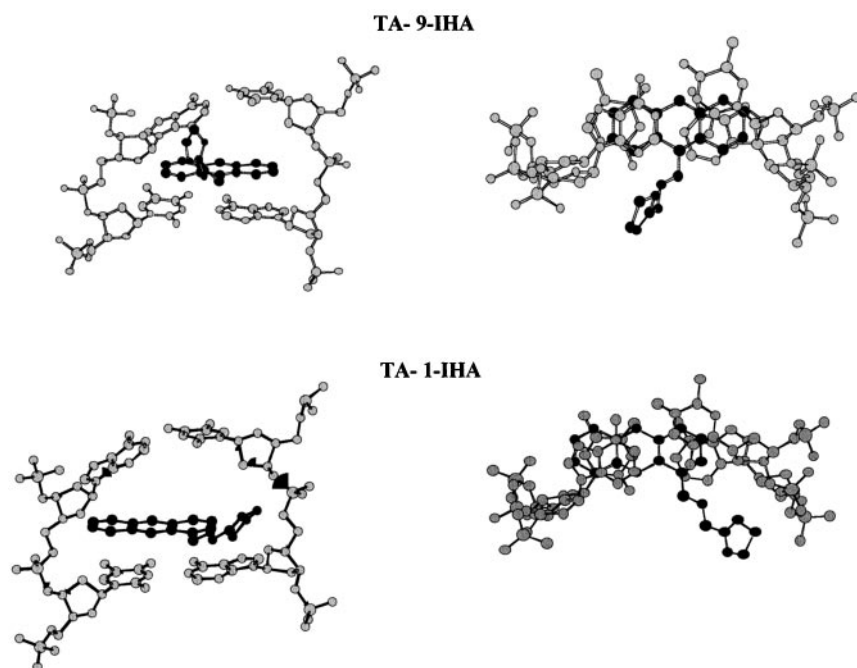
Fig. 6. Best intercalation geometries for intercalation of 9-IHA and 1-IHA into A-T base pairs, as obtained from the docking experiments. *Left*, view from the minor groove; *right*, view along the DNA axis. Hydrogen atoms are not shown. Atoms of the drug structure are in *black*.

and 7. In general, the side-chain groups protrude from the central part of the minor groove, producing effective electrostatic contacts with the negative charge density of the DNA. To optimize side-chain locations, the planar portions of the two drugs are considerably displaced in the intercalation pocket, with respect to each other. More efficient stacking interactions with A-T base pairs appear to be primarily responsible for the base preference exhibited by 9-IHA, compared with its 1-substituted isomer.

Discussion

The results obtained with the bisantrene congeners and presented here show unequivocally that the relative locations of the side chain and the planar ring system dramatically affect the affinity and specificity of these drugs for DNA. Loss of one of the two side chains of bisantrene clearly reduces binding to a major extent, which demonstrates the effective participation of both charged side-chain groups in the binding process. This is confirmed by the calculated value of 2 for the m' parameter (Table 2). The contribution of the dihydroimidazolyl lateral groups is not only electrostatic but must include noncharged contributions, as demonstrated by the $\Delta G°$ values extrapolated from the data measured at different ionic strengths. In fact, the $\Delta G°$ value for bisantrene is approximately 1 kcal/mol more negative than the $\Delta G°$ values for the 9-substituted analogues. The effects of bioisosteric substitution (C10 to N) essentially do not affect either K_i or $\Delta G°$. This indicates very similar arrangements of the planar moieties of 9-IHA and aza-9-IHA when the drugs are bound to DNA. On the other hand, a shift of the side chain from position 9 to position 1 reduces the interaction free energy (in absolute values) by an additional 1 kcal/mol ($\Delta G° \approx 5$ kcal/mol). Hence, less favorable contacts occur between the drug and DNA when the dihydroimidazolyl group is located on the lateral rings of anthracene. The melting experiment results are in agreement with these findings. Unfortunately, because of the self-aggregation and DNA-precipitating ability of 1,4-IHA, it was not possible to make a sound comparison between this compound and the isomer bisantrene.

Not only the binding thermodynamics are affected by a shift of the side chain to a different position; the DS is also dramatically changed with movement of the lateral group from position 9 to position 1. As shown in Table 5, the strong preference of the 9-substituted compounds for A-T base pairs vanishes with the 1-substituted drug. This is confirmed by the docking experiment results, which indicate a more stable intercalation into A-T pairs for 9-IHA and an essential loss of discrimination for A-T versus G-C steps by 1-IHA. Further elucidation of sequence specificity, which was attempted with footprinting studies, was only marginally successful because of the poor footprinting ability of the monosubstituted derivatives. Nevertheless, these experiments confirm a wider sequence acceptance exhibited by 1-IHA.

With elucidation of the effects of the chain shift, in terms of DS, it is interesting to observe that DS and TS coincide for the test drugs. Indeed, whereas the 9-substituted compounds confirm the A+1 preference of m-AMSA and bisantrene, the 1-substituted congener does not show any specificity in stimulating DNA cleavage (Capranico et al., 1998) (Table 1).

Recently, we have been interested in identification of the structural drug determinants for TS (Capranico et al., 1994; Palumbo et al., 1994). A key step in the enzyme-mediated mechanism of action is the formation of a ternary topoisomerase II-DNA-drug complex that establishes proper contacts between the drug pharmacophores and the enzyme and nucleic acid counterparts (Capranico et al., 1997). Although these contacts occur in a particular structure in which the original conformations of the macromolecular species are mutually distorted, some of the recognition features involved in binary drug-enzyme and drug-nucleic acid interactions should still be operative in the ternary system. In particular, for intercalating agents, the characteristics that allow preferential stacking onto given base pairs should also influence

CG- 9-IHA

CG- 1-IHA
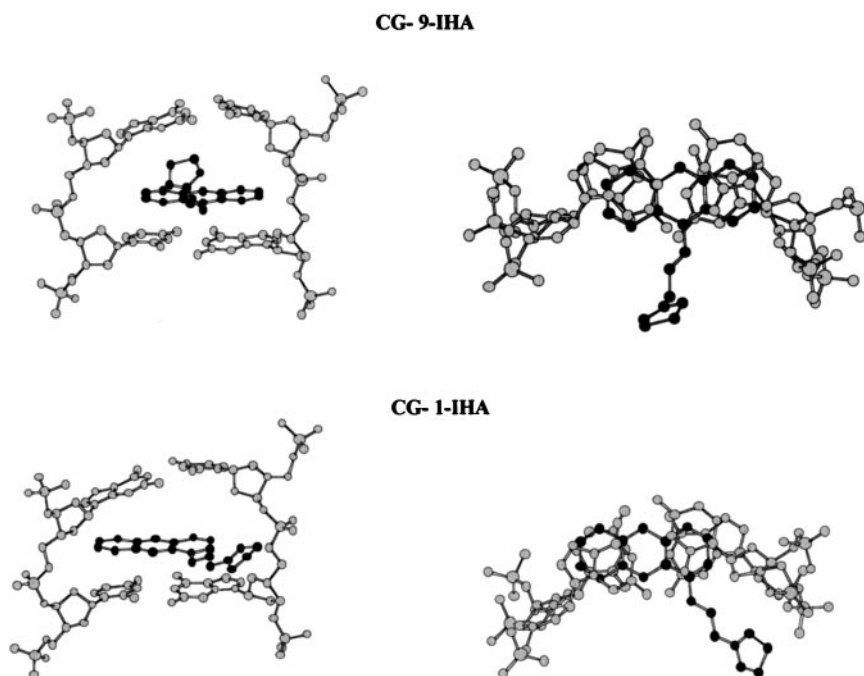
Fig. 7. Best intercalation geometries for intercalation of 9-IHA and 1-IHA into G-C base pairs, as obtained from the docking experiments. *Left*, view from the minor groove; *right*, view along the DNA axis. Hydrogen atoms are not shown. Atoms of the drug structure are in *black*.

the locations at which drug-mediated cleavage stimulation occurs.

In the case presented here, it appears that, notwithstanding the changes occurring in the cleavable complex, recognition of DNA by the drug is preserved as it was in the absence of the enzyme. This fact is confirmed by the parallel changes in DS and TS that occur when the drug structure is isomerized.

The finding that TS corresponds to DS for the test drugs is even more surprising when we consider that the +1 specificity involves the base directly linked to the catalytic tyrosine (Capranico *et al.*, 1997). Because of the special amino acid-nucleotide phosphodiester bond formed and the distortion caused by the new protein-linked arrangement, the base at +1 should be more profoundly affected (both electronically and structurally) than the base at position −1, with the latter remaining essentially paired in a double-helical conformation, as indicated by base-mismatch experiments (Bigioni *et al.*, 1996). Indeed, considering that the central portion of the cleavage region (positions +1 to +4) must be melted to allow DNA strand-passing and that it is the religation step that is mainly inhibited by drugs such as *m*-AMSA (Robinson and Osheroff, 1991), it is possible that compounds having +1 specificity stabilize a catalytic intermediate in which the target base is unpaired. This is in line with the aforementioned base-mismatch experiments (Bigioni *et al.*, 1996). In fact, whereas mismatches introduced at position −1, relative to the enzyme cleavage site, were shown to abolish DNA cleavage, those at positions +1 and +2 increased the level of DNA breakage instead. In the single-stranded region of DNA in the cleavable complex, the creation of efficient π interactions between the planar systems of the preferred base and of the drug should be crucial to avoid dissociation from the cleavable complex and loss of cleavage stimulation. Hence, efficient recognition of the DNA by the drug system through stacking interactions at position +1 in the cleavable complex should correlate with the base preferences in the enzyme-free system. This was, indeed, our observation. Moreover, the remarkable affinities shown by bisantrene and its congeners for stacking interactions with single-stranded DNA (Table 3) are consistent with the proposed recognition mechanism. In agreement with this concept, only purine bases, which exhibit an extended stacking surface, were previously found to be preferred for cleavage stimulation at position +1, whereas any base can be specifically recognized by different drugs at position −1 (Capranico *et al.*, 1997). Our model might also be effective for topoisomerase I poisons, as suggested by very recent work on the crystal structure of human topoisomerase I in covalent and noncovalent complexes with DNA (Redimbo *et al.*, 1998). In fact, based on chemical, structural, and biochemical evidence, the binding mode proposed for the anticancer drug camptothecin (exhibiting G+1 specificity) at the topoisomerase I-DNA complex suggests an effective stacking interaction of the guanine residue with the planar ring system of the drug. This is confirmed by the fact that TS corresponds to DS for indolocarbazole derivatives having +1 specificity (Bailly *et al.*, 1997, 1998).

From the aforementioned results, some useful insight can be gained into the molecular basis of the TS. It appears that, for +1-specific agents, the drug-DNA contacts are primarily responsible for base selectivity; the interaction between the protein and the poison does not play a major role in stabilizing a specific ternary complex intermediate. As a result, it should be possible to predict the likely location of +1 cleavage stimulation along the DNA chain from binary complex studies. As a corollary to the model presented here, a +1 cleavage-stimulating agent should be characterized by high affinity for single-stranded DNA. These findings have useful implications for the design of novel topoisomerase poisons. Studies on the DNA-binding properties of other topoisomerase II poisons exhibiting +1 specificity, such as saintopin (Leteurtre *et al.*, 1994) and NSC665517 [2-methyl-3-[2-(D-xylopyranosylamino)phenyl]-6,8-dibromo-4(^{3}H)-quinazolinone] (Gupta *et al.*, 1995) (both guanine specific), are warranted to confirm the general applicability of our model and further elucidate the mode of base selection in drug-stimulated DNA cleavage.

References

Bailly C, Colson P, Houssier C, Rodrigues Pereira E, Prudhomme M, and Waring MJ (1998) Recognition of specific sequences in DNA by a topoisomerase I inhibitor derived from the antitumor drug rebeccamycin. *Mol Pharmacol* **53:**77–87.

Bailly C, Denny WA, Mellor L, Wakelin LPG, and Waring MJ (1992) Sequence-specificity of the binding of 9-aminoacridine- and amsacrine-4-carboxamides to DNA studied by DNase I footprinting. *Biochemistry* **31:**3514–3524.

Bailly C, Riou JF, Colson P, Houssier C, Rodrigues Pereira E, and Prudhomme M (1997) DNA cleavage by topoisomerase I in the presence of indolocarbazole derivatives of rebeccamycin. *Biochemistry* **36:**3917–3929.

Bailly C and Waring MJ (1995) Comparison of different footprinting methodologies for detecting binding sites for a small ligand on DNA. *J Biomol Struct Dyn* **12:**869–898.

Berger JM, Gamblin SJ, Harrison SC, and Wang JC (1996) Structure and mechanism of DNA topoisomerase II. *Nature (Lond)* **379:**225–232.

Bigioni M, Zunino F, Tinelli S, Austin CA, Willmore E, and Capranico G (1996) Position-specific effects of base mismatch on mammalian topoisomerase II DNA cleaving activity. *Biochemistry* **35:**153–159.

Capranico G, Binaschi M, Borgnetto ME, Zunino F, and Palumbo M (1997) A protein-mediated mechanism for the DNA sequence-specific action of topoisomerase II poisons. *Trends Pharmacol Sci* **18:**323–329.

Capranico G, De Isabella P, Tinelli S, Bigioni M, and Zunino F (1993) Similar sequence specificity of mitoxantrone and VM-26 stimulation of *in vitro* DNA cleavage by mammalian DNA topoisomerase II. *Biochemistry* **32:**3038–3046.

Capranico G, Guano F, Moro S, Zagotto G, Sissi C, Gatto B, Menta E, Zunino F, and Palumbo M (1998) Mapping drug interactions at the topoisomerase II-DNA cleavable complex: studies on bisantrene-amsacrine analogues. *J Biol Chem* **273:** 12732–12739.

Capranico G, Kohn KW, and Pommier Y (1990) Local sequence requirements for DNA cleavage by mammalian topoisomerase II in the presence of doxorubicin. *Nucleic Acids Res* **18:**6611–6619.

Capranico G, Palumbo M, Tinelli S, Mabilia M, Pozzan A, and Zunino F (1994) Conformational drug determinants of the sequence specificity of drug-stimulated topoisomerase II DNA cleavage. *J Mol Biol* **235:**1218–1230.

Chen KX, Gresh N, and Pullman B (1988) Energetics and stereochemistry of DNA complexation with the anti-tumor AT specific intercalators tilorone and *m*-AMSA. *Nucleic Acids Res* **16:**3061–3073.

Crenshaw JM, Graves DE, and Denny WA (1995) Interactions of acridine antitumor agents with DNA: binding energies and groove preferences. *Biochemistry* **34:** 13682–13687.

De Isabella P, Capranico G, Binaschi M, Tinelli S, and Zunino F (1990) Evidence of DNA topoisomerase II-dependent mechanisms of multidrug resistance in P388 leukemia cells. *Mol Pharmacol* **37:**11–16.

Denny WA and Wakelin LP (1987) Mode and kinetics of DNA binding of the anti-tumour agent bisantrene. *Anticancer Drug Design* **2:**71–77.

Foye WO, Karnik PS, and Sengupta SK (1986) DNA-binding abilities of bisguanyl-hydrazones of anthracene-9,10-dicarboxaldehyde. *Anticancer Drug Design* **1:**65–71.

Frederick CA, Williams LD, Ughetto G, Van Der Marel GA, Van Boom JH, Rich A, and Wang AH-J (1990) Structural comparison of anticancer drug-DNA complexes: Adriamycin and daunomycin. *Biochemistry* **29:**2538–2549.

Freudenreich CH and Kreuzer KN (1994) Localization of an aminoacridine antitumor agent in a type II topoisomerase-DNA complex. *Proc Natl Acad Sci USA* **91:**11007–11011.

Grant RC, Harwood SJ, and Wells RD (1968) The synthesis and characterization of poly d(I-C)·poly d(I-C). *J Am Chem Soc* **90:**4474–4476.

Gupta M, Abdel-Megeed M, Hoki Y, Kohlhagen G, Paull K, and Pommier Y (1995) Eukaryotic DNA topoisomerases mediated DNA cleavage induced by a new inhibitor, NSC 665517. *Mol Pharmacol* **48:**658–665.

Hehre WJ, Radom L, Schleyer PVR, and Pople JA (1986) *Ab Initio Molecular Orbital Theory.* John Wiley and Sons, New York.

Leteurtre F, Fujimori A, Tanizawa A, Chhabra A, Mazumder A, Kohlhagen G, Nakano H, and Pommier Y (1994) Saintopin, a dual inhibitor of DNA topoisomerases I and II, as a probe for drug-enzyme interactions. *J Biol Chem* **269:**28702–28707.

Leteurtre F, Madalengoitia J, Orr A, Guzi TJ, Lehnert E, Macdonald T, and Pom-

mier Y (1992) Rational design and molecular effects of a new topoisomerase II inhibitor, azatoxin. *Cancer Res* **52:**4478–4483.

Liu LF (1989) DNA topoisomerase poisons as antitumor drugs. *Annu Rev Biochem* **58:**351–375.

McGhee JD and Von Hippel PH (1974) Theoretical aspects of DNA-protein interactions: cooperative and noncooperative binding of large ligands to a one-dimensional homogeneous lattice. *J Mol Biol* **86:**469–489.

Mohamadi F, Richards NGJ, Guida WC, Liskamp R, Lipton M, Caufield C, Chang G, Hendrickson T, and Still WC (1990) Macromodel: an integrated software system for modeling organic and bioorganic molecules using molecular mechanics. *J Comput Chem* **11:**440–450.

Neidle S, Pearl LH, Herzyk P, and Berman HM (1988) A molecular model for proflavine-DNA intercalation. *Nucleic Acids Res* **16:**89–99.

Osheroff N, Corbett AH, Elsea SH, and Westergaard M (1994) Defining functional drug-interaction domains on topoisomerase II by exploiting mechanistic differences between drug classes. *Cancer Chemother Pharmacol* **34**(Suppl)**:**S19–S25.

Palumbo M, Capranico G, Tinelli S, Mabilia M, Pozzan A, and Zunino F (1994) Conformational properties of topoisomerase II inhibitors and sequence specificity of DNA cleavage. *J Mol Recognition* **7:**227–231.

Pommier Y (1993) DNA topoisomerase I and II in cancer chemotherapy: update and perspectives. *Cancer Chemother Pharmacol* **32:**103–108.

Pommier Y, Capranico G, Orr A, and Kohn KW (1991) Local base sequence preferences for DNA cleavage by mammalian topoisomerase II in the presence of amsacrine or teniposide. *Nucleic Acids Res* **19:**5973–5980.

Record MT Jr, Anderson CF, and Lohman TM (1978) Thermodynamic analysis of ion effects on the binding and conformational equilibria of proteins and nucleic acids: the roles of ion association on release, screening, and ion effects on water activity. *Q Rev Biophys* **11:**103–178.

Redimbo MR, Lance S, Kuhn P, Champoux JJ, and Hol WGJ (1998) Crystal structure of human topoisomerase I in covalent and noncovalent complexes with DNA. *Science (Washington DC)* **279:**1504–1513

Robinson MJ and Osheroff N (1991) Effects of antineoplastic drugs on the post-strand-passage DNA cleavage/religation equilibrium of topoisomerase II. *Biochemistry* **30:**1807–1813.

Schwartz G, Klose S, and Baltasan W (1970) Cooperative binding to linear biopolymers. 2. Thermodynamic analysis of the proflavine-poly(L-glutamic acid) system. *Eur J Biochem* **12:**454–460.

Wakelin LPG, Chetcuti P, and Denny WA (1990) Kinetic and equilibrium binding studies of amsacrine-4-carboxamides: a class of asymmetrical DNA-intercalating agents which bind by threading through the DNA helix. *J Med Chem* **33:**2039–2044.

Weiner SJ, Kollman PA, Nguyen DT, and Case DA (1986) An all-atom force field for simulation of protein and nucleic acids. *J Comput Chem* **7:**230–252.

Wells RD, Larson JE, Grant RC, Shortle BE, and Cantor CR (1970) Physicochemical studies on polydeoxyribonucleotides containing defined repeating nucleotide sequences. *J Mol Biol* **54:**465–497.

Wunz TP, Craven MT, Karol MD, Hill GC, and Remers WA (1990) DNA binding by antitumor anthracene derivatives. *J Med Chem* **33:**1549–1553.

Zagotto G, Oliva A, Guano F, Menta E, Capranico G, and Palumbo M (1998) Synthesis, DNA-damaging and cytotoxic properties of novel topoisomerase II-directed bisantrene analogues. *Bioorg Med Chem Lett* **8:**121–126.

Send reprint requests to: Dr. Manlio Palumbo, Department of Pharmaceutical Sciences, University of Padova, Via Marzolo 5, 35131 Padova, Italy. E-mail: mpalumbo@purple.dsfarm.unipd.it